Terahertz Wireless Communications Using Resonant Tunneling Diodes as Transmitters and Receivers

Tadao Nagatsuma, Masayuki Fujita, Ai Kaku, Daiki Tsuji, and Shunsuke Nakai
Graduate School of Engineering Science, Osaka University,
1-3 Machikaneyma, Toyonaka 560-8531, Japan
nagatuma@ee.es.osaka-u.ac.jp

Kazuisao Tsuruda, and Toshikazu Mukai
Photonics R&D Center, Rohm Co., Ltd.,
21 Saiin Mizosaki-cho, Ukyo-ku, Kyoto 615-8585, Japan

Keywords: Terahertz, communication, resonant tunneling diode, transmitter, receiver, transceiver

Abstract: This paper presents a transceiver module employing a resonant tunneling diode (RTD), which can be operated as both a transmitter and a receiver just by changing the bias voltages. Error-free wireless transmission experiments have successfully been demonstrated at 300 GHz at bit rates of 10 Gbit/s and 2.5 Gbit/s by using an RTD receiver and a transceiver, respectively.

1 INTRODUCTION

Recently, there has been an increasing interest in the application of terahertz (THz) waves (0.1 THz ~ 10 THz) to the ultrahigh-speed wireless communications. In particular, the use of carrier frequencies above 275 GHz is one of the strong attentions among radio scientists and engineers, because these frequency bands have not yet been allocated to specific active services, and there is a possibility to employ extremely large bandwidths for ultra-broadband wireless communications (Kleine-Ostmann and Nagatsuma, 2011, Song and Nagatsuma, 2011).

A 300-GHz band wireless link at a bit rate of over 40 Gbit/s has been reported, in which a photonics-based transmitter and a Schottky-barrier diode (SBD) detector are used (Nagatsuma et al., 2013). To bring the THz wireless communications technology to a widespread consumer marketplace, the development of transmitters based on compact semiconductor electronic devices is urgently required. Among various semiconductor electronic devices and integrated circuits, resonant tunneling diodes (RTDs) have exhibited the highest oscillation frequency at over 1 THz (Asada et al., 2008, Suzuki et al., 2010). In this paper, we first describe the application of RTDs to receivers in THz wireless communications. Sensitivity enhancement due to strong nonlinearity of direct current (DC) current-voltage (I-V) characteristics is discussed both theoretically and experimentally. Receiver modules integrated with an MgO lens are developed for broadband operation at a bit rate of over 10 Gbit/s with a carrier frequency of 300 GHz. Finally, multi-gigabit wireless transmission experiments are demonstrated using RTDs as both the transmitter and receiver at 300 GHz.

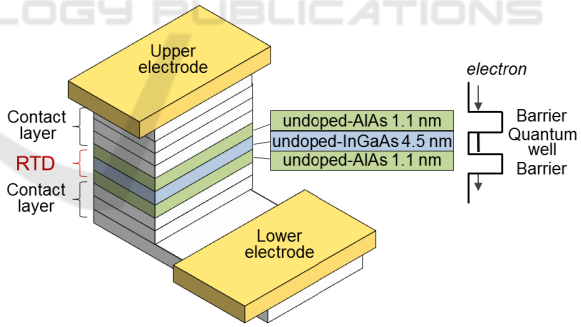

Figure 1: Typical device layer structure of RTD.

2 DEVICE STRUCTURES AND OPERATION PRINCIPLE

Figure 1 shows a typical device layer structure of the RTD on InP substrate. The resonant tunneling region of the diode is composed of an InGaAs/AlAs double barrier structure. By making upper and lower contact layers asymmetric, DC I-V characteristics become

Nagatsuma T., Fujita M., Kaku A., Tsuji D., Nakai S., Tsuruda K. and Mukai T.
Terahertz Wireless Communications Using Resonant Tunneling Diodes as Transmitters and Receivers.
DOI: 10.5220/0005421000410046
In *Proceedings of the Third International Conference on Telecommunications and Remote Sensing (ICTRS 2014)*, pages 41-46
ISBN: 978-989-758-033-8

asymmetric with a polarity of DC voltage or current as shown in Fig. 2. A wide negative resistance (NDR) region (Point A) is suitable to the oscillator operation, while the peak point with the opposite polarity (Point B) is appropriate for the detector operation.

Usually, the RTD is integrated with a planar antenna such as dipole and tapered slot antennas. The antenna-integrated RTD chip is mounted on the coplanar waveguide substrate with the co-axial connector via bonding wire as shown in Fig. 3.

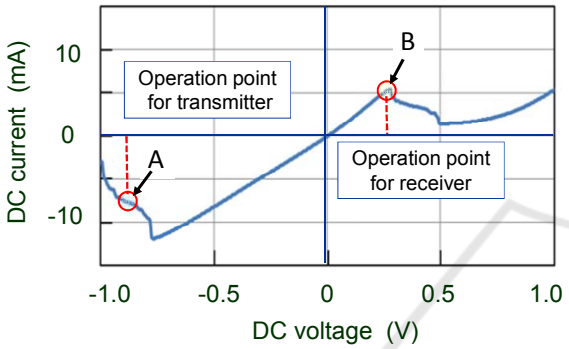

Figure 2: DC I-V characteristics of the RTD and operation points for transmitter (A) and receiver (B).

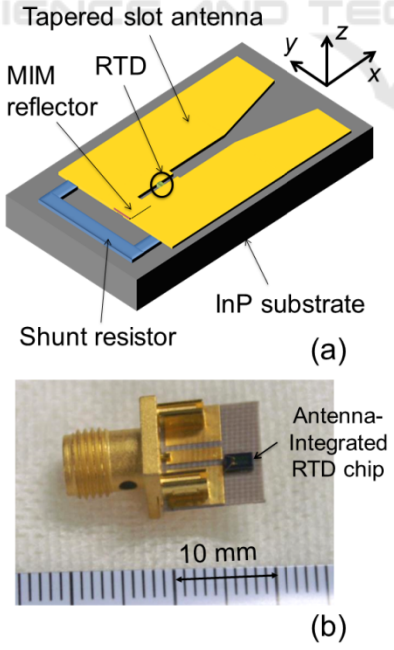

Figure 3: (a) Schematic of antenna-integrated RTD. (b) Photograph of a connectorised RTD module.

3 APPLICATIONS TO RECEIVERS

3.1 Responsivity Evaluation

Receiver responsivity can be estimated from DC I-V characteristics based on the square-low detection theory (Cowley and Sorenson, 1966). The detected power is expressed in the case of 50-ohm load as

$$P = \left\{ \frac{\left(A^2/4\right) f^{(2)}(V_{Bias}) + \left(A^4/64\right) f^{(4)}(V_{Bias})}{f^{(1)}} \right\}^2 \Big/ 50 \qquad (1),$$

where $f(V)$ $(= I)$ is the I-V function, $f^{(1)}$, $f^{(2)}$, and $f^{(4)}$ are derivatives of $f(V)$ with respect to V, and A is an amplitude of the input radio frequency (RF) voltage applied to the RTD.

We have conducted the experiment to verify the above theory by using the receiver module, where the RTD chip is bonded to a tapered slot antenna on a glass epoxy substrate (FR-4) as shown in Fig. 4. In order to evaluate an intrinsic responsivity of the RTD avoiding the influence of a conductor loss and parasitic elements, 35-GHz signals were received by the module with the RTD chip which has a cut-off frequency above 300 GHz. 35-GHz signals were amplitude-modulated at 100 kHz, and demodulated signals by the receiver was measured by a spectrum analyzer tuned at 100 kHz.

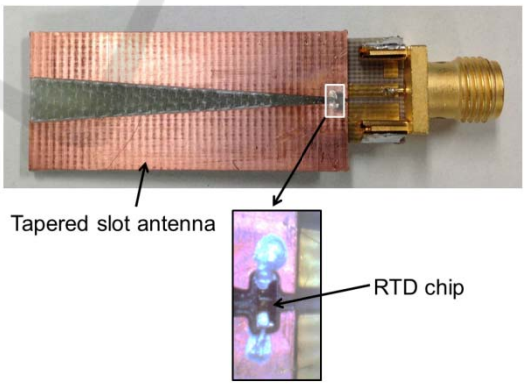

Figure 4: Photograph of the RTD receiver module for 35-GHz experiment.

Figure 5 shows a dependence of the received power measured as a function of the DC bias voltage. The DC I-V characteristics are also plotted in the figure. A solid line (measured) and a broken one (calculated) agree quite well. Relative responsivity

becomes maximum at the peak voltage just before the NDR region as expected. In the NDR region, the output voltage becomes unstable and a noise level increases.

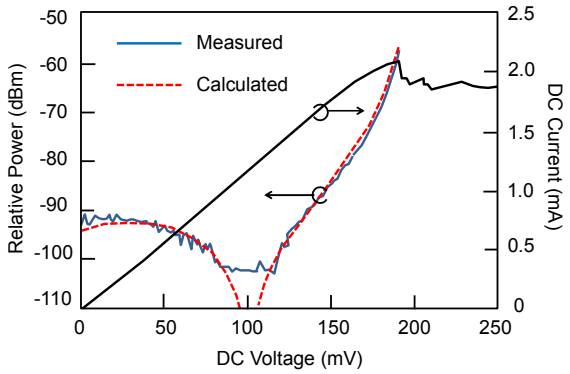

Figure 5: Relative responsivity and DC current as a function of DC bias voltage.

3.2 Receiver Modules

We simulated antenna radiation patterns of the RTD chip of Fig. 3(a) (1.9 mm long, 0.9 mm wide and 0.6 mm thick) for frequencies of 295 GHz, 300 GHz, and 305 GHz, by finite-difference time-domain (FDTD) method as shown in Fig. 6. Due to relatively thick InP substrate with a high relative dielectric constant, ε_r (12.1), the radiation patterns become diverse and vary considerably with the frequency. The electromagnetic waves do not propagate along the tapered slot antenna, but are attracted into the InP substrate (Yngveson et al., 1989), which results in Fabry-Perot resonance inside the substrate, and a maximum antenna gain of 8.8 dBi.

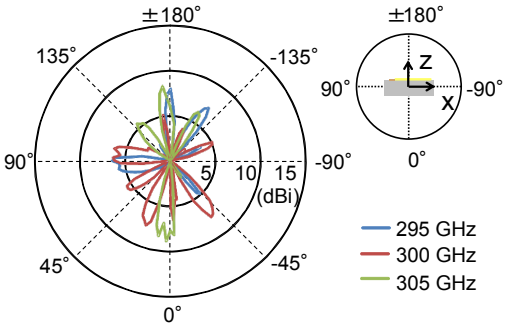

Figure 6: Simulated antenna patterns on H-plane of the RTD chip shown in Fig. 3 for various frequencies.

We examined an integration of an MgO hyper-hemispherical lens (Nakajima et al., 2004) with the RTD chip in order to improve the antenna pattern. Attaching a hyper-hemispherical lens to substrate can lead to the efficient coupling of THz radiation to the free space from the substrate with a collimation effect and low aberration (Van Rudd et al., 2002). The reflection at the InP-MgO interface is small since the relative dielectric constant of MgO is $\varepsilon_r \sim 9.7$ for 300 GHz, which is close to that of the InP substrate. MgO is almost transparent both for THz waves and visible light. Thus we can easily integrate the lens while aligning the position of the RTD chip. The chip is glued to the center of the cross-section of the lens by ultraviolet cure adhesive. Figure 7 shows the simulated antenna patterns of the RTD chip integrated with the MgO lens. The directivity is almost the same for 290–300 GHz. The maximum antenna gain is 12.5 dBi.

Figure 8 shows photographs of the RTD receiver module with the MgO lens.

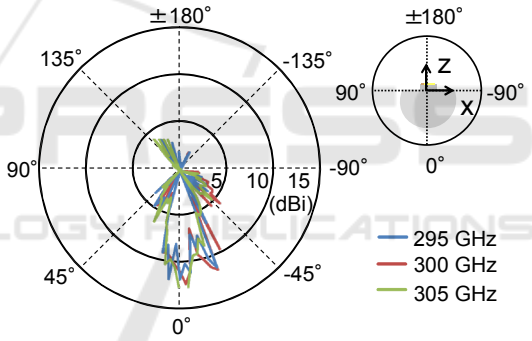

Figure 7: Simulated antenna patterns on H-plane of the RTD chip with MgO lens for various frequencies.

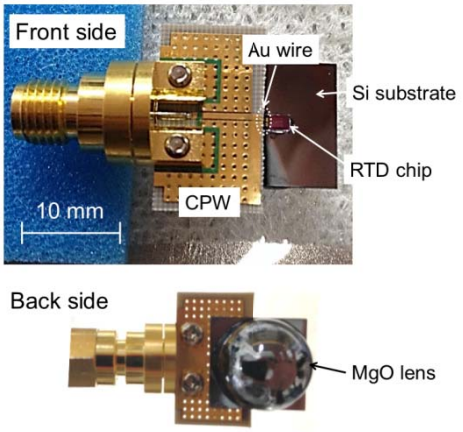

Figure 8: Photographs of the RTD receiver module with MgO lens.

We conducted wireless transmission experiments using a frequency-multiplier-based transmitter and the RTD receiver. Figure 9 depicts a schematic diagram of the experimental setup. The output signal from the up-converter, which mixes the RF signal from a synthesizer (32–36 GHz) and the digital signal from a pulse-pattern generator, is multiplied by nine times to generate THz signals at 288–324 GHz. THz signals are radiated into the free space by a horn antenna (25 dBi), and are detected by the RTD receiver module. Demodulated signals are amplified and re-shaped by a preamplifier and a limiting amplifier, respectively.

Figure 10 shows bit error rate (BER) characteristics and eye diagrams. Error-free ($BER<10^{-11}$) transmission has been confirmed up to the bit rate of about 11 Gbit/s. Currently, the maximum bit rate is limited by the modulation bandwidth of the transmitter based on the frequency multiplier. Our design of the receiver module ensures the bit rate of over 20 Gbit/s.

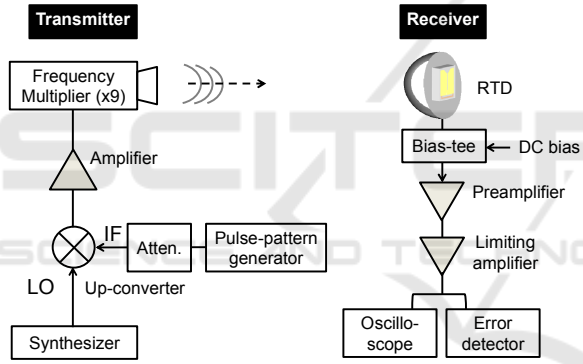

Figure 9: Block diagram of wireless transmission experiment using a frequency-multiplier-based transmitter and the RTD receiver.

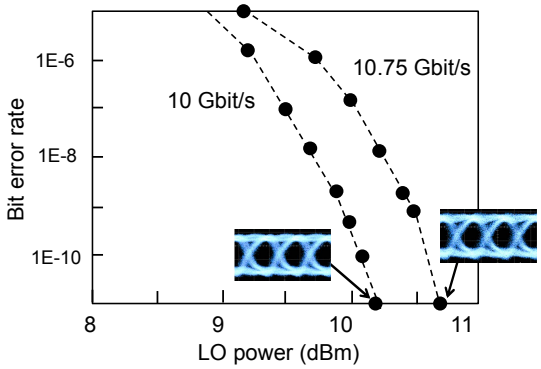

Figure 10: Bit error rate characteristics and eye diagrams at 300 GHz.

4 APPLICATIONS TO ALL RTD-BASED TRANSCEIVERS

For the operation of the RTD as a transmitter, the amplitude of the applied voltage is changed to perform the on-off keying (OOK) modulation as shown in Fig. 11. The amplitude of both the DC bias and RF modulation voltages was carefully adjusted so that the output power from the RTD became maximum (Mukai et al., 2011).

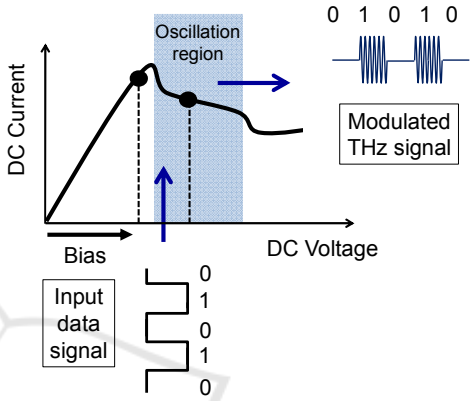

Figure 11: Operation of the RTD as a transmitter with OOK modulation scheme.

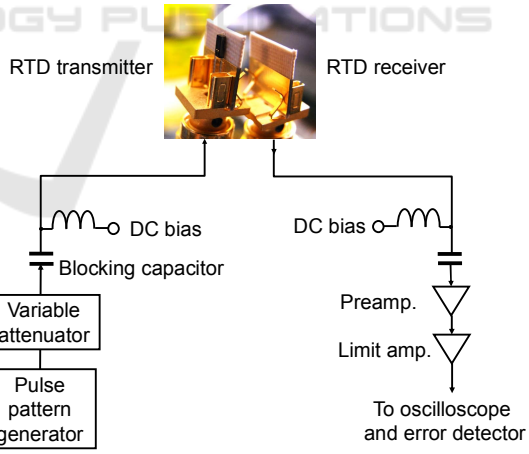

Figure 12: Experimental setup of proximity wireless transmission experiment using two sets of RTD modules.

By using two sets of RTD modules without MgO lens (Fig. 3(b)), we conducted a close-proximity wireless transmission experiment, placing the two modules at a distance from a few millimeters to several tens of millimeters as shown in Fig. 12. For

the transmitter, the data signal (RF voltage) from the pulse-pattern generator was applied to the module with an appropriate DC bias voltage through a bias-T. For the receiver, just a DC bias voltage was applied to the RTD to maximize the sensitivity. The demodulated baseband data signal was amplified with the preamplifier followed by the limiting amplifier.

The oscillation frequency depends on the parallel inductance and capacitance of RTD chip, and the output power is proportional to the widths of the current and voltage of the NDR region (Asada et al., 2008). The oscillation frequency and the output power of the RTD used for the experiments were approximately 300 GHz and several μW, respectively.

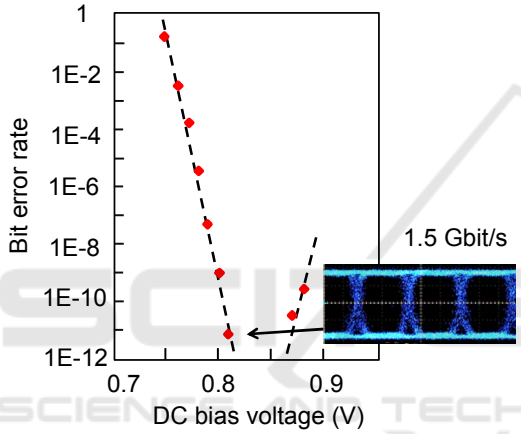

Figure 13: BER characteristics plotted against the DC bias voltage and eye diagram at 1.5 Gbit/s.

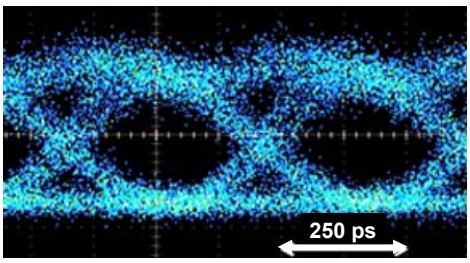

Figure 14: Demodulated eye diagram at 2.5 Gbit/s.

Figure 13 shows a dependence of the BER on the applied DC bias voltage when the amplitude of the data signal was 160 mVp-p. At 0.85 V, an error-free transmission at 1.5 Gbit/s was achieved as shown in the eye diagram of Fig. 13. There were optimum DC bias voltages depending on the RF voltage amplitude. By carefully adjusting the DC bias voltage, the achieved maximum data rate was 2.5 Gbit/s (Fig. 14), which is mainly limited by the frequency-dependent radiation pattern as discussed in Sec. 3.2, and the bandwidth of the packaging (Shiode et al., 2011, 2012). Use of RTD transceiver modules with MgO lens will increase the bit rate over 10 Gbit/s.

5 CONCLUSIONS

We have described a small and cost-effective transceiver module employing resonant-tunnelling diodes (RTDs) towards wide-spread consumer THz wireless applications such as a close-proximity instantaneous data transfer and a wireless interconnection.

The RTD-based receiver module with MgO hyper-hemispherical lens has exhibited over 10-Gbit/s performance at 300 GHz. Using the RTD-based transmitter and receiver, a close-proximity wireless transmission at 2.5 Gbit/s has been demonstrated with an error-free condition. Future works should be placed on the increase of data rate and transmission distance by improving the packaging and the antenna structure, respectively.

ACKNOWLEDGEMENT

This work was supported in part by the Strategic Information and Communications R&D Promotion Programme (SCOPE), from the Ministry of Internal Affairs and Communications, Japan.

REFERENCES

Asada, M., Suzuki S., Kishimoto, N., 2008. Resonant tunneling diodes for sub-terahertz and terahertz oscillators. *Jpn. J. Appl. Phys*., Vol. 47, No. 6, pp. 4375–4384, 2008.

Cowley A. M., Sorenson, H. O., 1966. Quantitative comparison of solid-state microwave detectors. *IEEE Trans. Microwave Theory and Tech.*, vol. 14, pp. 588–602.

Kleine-Ostmann, T., Nagatsuma, T., 2011. A review on terahertz communications research. *J. Infrared Milli. Terhz. Waves*, vol. 32, no. 2, pp. 143–171.

Mukai T., M. Kawamura, M., Takada, T., Nagatsuma, T., 2011. 1.5-Gbps wireless transmission using resonant tunneling diodes at 300 GHz. *Tech. Dig. Optical Terahertz Science and Technology (OTST2011)*, MF42, Santa Barbara.

Nagatsuma, T., Ito, H., Ishibashi, T., 2009. High-power RF photodiodes and their applications. *Laser Photon. Rev.*, vol. 3, no. 1-2, pp. 123–137.

Nagatsuma, T. et al., 2013. Terahertz communications based on photonics technologies, *Optics Express*, vol. 21, no. 20, pp. 23736–23747.

Nakajima, M., Uchida, K., Tani, M., Hangyo, M., 2004. Strong enhancement of terahertz radiation from semiconductor surfaces using MgO hemispherical lens coupler. *Appl. Phys. Lett.*, vol. 85, no. 2, pp. 191–193.

Shiode, T., Mukai, T., Kawamura, M., Nagatsuma, T., 2011. Giga-bit wireless communication at 300 GHz using resonant tunneling diode detector. *Proc. Asia-Pacific Microwave Conference (APMC2011),* Melbourne.

Shiode, T., Kawamura, M., Mukai, T., Nagatsuma, T., 2012. Resonant-tunneling diode transceiver for 300 GHz-band wireless link. *Tech. Dig. Asia-Pacific Microwave Photonics Conf. (APMP2012)*, WC-1, Kyoto.

Song, H.-J., Nagatsuma, T., 2011. Present and future of terahertz communications. *IEEE Trans. Terahertz Science and Technology*, vol.1, no. 1, 256–264.

Suzuki, S., Asada, M., Teranishi, A., Sugiyama H., Yokoyama, H., 2010. Fundamental oscillation of resonant tunneling diodes above 1 THz at room temperature. *Applied Physics Letters*, vol. 97, no. 24, pp. 242102–242102-3.

Van Rudd J., Mittleman, D. M., 2002. Influence of substrate-lens design in terahertz time-domain spectroscopy. *J. Opt. Soc. Am. B*, vol. 19, no. 2, pp. 319–328.

Yngveson, K. S., Korzeniowski, T. L., Kim, Y.-S., Kollberg, E. L., Johansson, J. F., 1989. The tapered slot antenna- A new integrated element for millimeter-wave applications. *IEEE Trans. Microwave Theory and Tech.*, vol. 37, no. 2, pp. 365–374.